Journal of Hydrology 526 (2015) 287–302

Contents lists available at ScienceDirect

Journal of Hydrology

journal homepage: www.elsevier.com/locate/jhydrol

Comparison of satellite-derived LAI and precipitation anomalies over Brazil with a thermal infrared-based Evaporative Stress Index for 2003–2013

Martha C. Anderson [a,*], Cornelio A. Zolin [b], Christopher R. Hain [c], Kathryn Semmens [d], M. Tugrul Yilmaz [e], Feng Gao [a]

[a] USDA-ARS, Hydrology and Remote Sensing Laboratory, Beltsville, MD, United States
[b] Embrapa Agrosilvopastoral, Sinop, MT, Brazil
[c] Earth System Science Interdisciplinary Center, University of Maryland, College Park, MD, United States
[d] Nature Nurture Center, Easton, PA, United States
[e] Middle East Technical University, Civil Engineering Department, Water Resources Division, Ankara, Turkey

ARTICLE INFO

Article history:
Available online 12 February 2015

Keywords:
Evapotranspiration
Drought
Remote sensing
Brazil
Amazon

SUMMARY

Shortwave vegetation index (VI) and leaf area index (LAI) remote sensing products yield inconsistent depictions of biophysical response to drought and pluvial events that have occurred in Brazil over the past decade. Conflicting reports of severity of drought impacts on vegetation health and functioning have been attributed to cloud and aerosol contamination of shortwave reflectance composites, particularly over the rainforested regions of the Amazon basin which are subject to prolonged periods of cloud cover and episodes of intense biomass burning. This study compares timeseries of satellite-derived maps of LAI from the Moderate Resolution Imaging Spectroradiometer (MODIS) and precipitation from the Tropical Rainfall Mapping Mission (TRMM) with a diagnostic Evaporative Stress Index (ESI) retrieved using thermal infrared remote sensing over South America for the period 2003–2013. This period includes several severe droughts and floods that occurred both over the Amazon and over unforested savanna and agricultural areas in Brazil. Cross-correlations between absolute values and standardized anomalies in monthly LAI and precipitation composites as well as the actual-to-reference evapotranspiration (ET) ratio used in the ESI were computed for representative forested and agricultural regions. The correlation analyses reveal strong apparent anticorrelation between MODIS LAI and TRMM precipitation anomalies over the Amazon, but better coupling over regions vegetated with shorter grass and crop canopies. The ESI was more consistently correlated with precipitation patterns over both landcover types. Temporal comparisons between ESI and TRMM anomalies suggest longer moisture buffering timescales in the deeper rooted rainforest systems. Diagnostic thermal-based retrievals of ET and ET anomalies, such as used in the ESI, provide independent information on the impacts of extreme hydrologic events on vegetation health in comparison with VI and precipitation-based drought indicators, and used in concert may provide a more reliable evaluation of natural and managed ecosystem response to variable climate regimes.

1. Introduction

Droughts and pluvials are normal and recurring climatic phenomena that affect people and the landscapes they occupy at many scales (locally, regionally, and nationally) for periods of time varying from weeks to decades. The spatial and temporal variability and multiple impacts of moisture anomalies at both extremes present challenges for mapping and monitoring over this range of scales. In the past decade, Brazil has experienced major drought events resulting in profound social, environmental and economic impacts which have raised great interest and concern in the scientific community and within government institutions engaged in monitoring and mitigation. Because Brazil is a major producer and exporter of soybean, corn, and cotton, realtime monitoring of impacts on Brazilian agricultural production is also important from a global market standpoint. In addition, there is ever-growing interest in monitoring impacts of changing climate on the health and resilience of Brazilian forested lands, which constitute a major fraction of the Amazon rainforest.

* Corresponding author at: 10300 Baltimore Ave, Beltsville, MD 20705, United States.
E-mail address: martha.anderson@ars.usda.gov (M.C. Anderson).

http://dx.doi.org/10.1016/j.jhydrol.2015.01.005
0022-1694/Published by Elsevier B.V.

Major droughts in Brazil over the past decade include events in Amazonia during 2005 and 2010, and in northeast Brazil in 2012–2013. In 2005, a 40-year low in river levels (14.75 m) was measured in the Rio Negro recorded at Manaus in central Amazonia, superseded in 2010 by the lowest river level (13.63 m) ever recorded (Marengo et al., 2008, 2011). These events significantly affected waterborne transportation, agriculture, generation of hydroelectricity, food security and human health along the rivers of the region. Commensurate with these drought events was an increase in wildfire outbreaks, with damage to vast areas of forest as well as production of dense smoke affecting human health and closing airports (Marengo et al., 2008). Ongoing severe (50-year) drought events in northeast Brazil in 2012–2013 have impacted more than 1400 municipalities (Leivas et al., 2012; Marengo et al., 2013a), leading to a declaration of a state of public calamity and the import of water supplies by truck.

Rapid onset drought events, or "flash droughts", afflicted the southern region of Brazil in 2005, 2009 and 2012. Such events have little lead warning time, and can result in significant financial loss. According to Agencia Brasil (Brazil Agency), the 2012 "flash drought" resulted in agricultural losses exceeding 2 billion reais (approximately $870 million) in southern Brazil and more than 800 million reais ($348 million) for the Agricultural Activities Guarantee Programme (Proagro), according to the Department of Rural Credit and Proagro of the Central Bank. In Rio Grande do Sul (one of the three states in the south region), 34% of grain production was lost in 2012 due to drought (FARSUL, 2013).

While agriculture has clearly borne major impacts with quantifiable economic ramifications, most drought/flood research in Brazil has focused on ecological aspects relating to the Amazon rainforest (Chen et al., 2010; Coelho et al., 2012; Espinoza et al., 2012; Hastenrath et al., 1984; Lewis et al., 2011; Liu et al., 1994; Marengo et al., 2013a, 2013b, 2008, 2011; Moura and Shukla 1981; Phillips et al., 2009; Saleska et al., 2007; Samanta et al., 2010a). Conclusions from these studies regarding the resilience of rainforest to rainfall extremes have been mixed, with some results suggesting that drought-induced stress in 2005 led to increased vigor in green vegetation cover as indicated by satellite vegetation indices (VIs) (Saleska et al., 2007). Others have not been able to reproduce these findings, and suggest incomplete treatment of aerosol/clouds in the Moderate Resolution Imaging Spectroradiometer (MODIS) VI products used created spurious anticorrelations between precipitation and VI anomalies (Samanta et al., 2010a).

Such great social, environmental and economic impacts caused by droughts and floods in Brazil have led government institutions to seek new and dynamic approaches to monitoring the severity of these natural events, as well as to serve as a tool to support decision makers in mitigating drought impacts. Currently, only a few federal institutions provide proxy information regarding drought conditions at the national scale (e.g. the Agrometeorological Monitoring System – Agritempo, the National Institute of Meteorology – INMET, and the National Institute for Space Research – INPE). Much of this monitoring relies on the existing rain gauge network, largely installed over the past 10–15 years and with some limitations in sampling density – particularly in north-central Brazil. This lack of high quality precipitation data presents a significant challenge for national drought and flood monitoring capabilities. Available stream gauge datasets provide valuable long-term information for major river systems, but it is difficult to extrapolate these point measurements to broader spatial coverage.

In the face of these data needs, operational satellite-based hydrologic monitoring can provide valuable spatial context for interpreting national in-situ precipitation and streamgauge datasets (Wardlow et al., 2012). Of specific relevance to monitoring anomalies in agricultural water use and ecosystem health are techniques based on remote sensing of evapotranspiration (ET) using satellite-derived maps of landsurface temperature (LST) retrieved from thermal infrared (TIR) imagery (Anderson et al., 2012a, 2013, 2011a, 2011b). LST is a diagnostic indicator of both surface energy balance, including evaporative fluxes (the latent heat flux in units of W m^{-2}, or ET in terms of mass loss in mm d^{-1}), and vegetation stress as expressed through enhanced canopy temperatures. In recent rapid drought onset events occurring over the United States, the Evaporative Stress Index (ESI), representing standardized anomalies in the ratio of TIR-based ET to reference ET (f_{RET}), provided advanced warning – often by more than 4 weeks – of significant degradation in drought severity classification reported in the United States Drought Monitor (Anderson et al., 2013; Otkin et al., 2013a, 2013b). In comparisons over the continental U.S., Hain et al. (2012, 2011) found that TIR retrievals of f_{RET} provided useful proxy information about rootzone soil moisture conditions under dense vegetation – areas where microwave soil moisture retrievals typically fail. These findings suggest utility for ESI in terms of timely assessments of drought impacts and soil water availability at national scales, over strongly heterogeneous landscapes.

The purpose of this paper is to evaluate the performance of the ESI in its first application outside the continental U.S., with specific focus on assessing differences in index response over forested and agricultural lands in Brazil. We compare ESI behavior over this domain with that of two principal drivers of the reference ET ratio (f_{RET}) describing consumptive water use: precipitation (water supply) and green biomass (water consuming agent) as quantified by the Leaf Area Index (LAI). Because the ET estimates used in the ESI are diagnosed via LST and energy balance rather than water balance, the ESI provides independent confirmation of emerging drought signals in comparison with precipitation-related indices typically used in drought monitoring, and potentially at much higher spatial resolution (Yilmaz et al., 2014). LAI is functionally related to shortwave vegetation indices such as the Normalized Difference Vegetation Index (NDVI) or Enhanced Vegetation Index (EVI), which have also frequently been used to assess drought impacts over the Amazon region as discussed above but with somewhat ambiguous conclusions.

In this paper, ESI computed over a baseline from 2003 to 2013 is compared to anomalies in rainfall derived from Tropical Rainfall Measuring Mission (TRMM) data and in LAI products from MODIS (Collection 5). TRMM precipitation and MODIS vegetation products have been staples in many existing studies of Amazonian vegetation and drought dynamics (e.g., Anderson et al., 2010; Doughty and Goulden, 2008; Lewis et al., 2011; Myneni et al., 2007; Saleska et al., 2007; Samanta et al., 2012), and therefore serve as well-established benchmarks for comparison. These satellite mapping products and derived anomalies are first compared at the continental scale over South America to provide spatial and historical context over the past decade. Then, relative response in product anomalies to major drought and flood events in Brazil from 2003 to 2013 is examined, as well as variability in temporal coupling between indices in different vegetation zones.

2. Study area

ESI, TRMM and MODIS LAI datasets have been assembled over a grid with $0.1 \times 0.1^{\circ}$ (nominally 10×10 km) spatial resolution covering the South American continent (see extent in Fig. 1a). Within this region, the focus is primarily on impacts observed in the country of Brazil, although maps are shown over the full continent to provide spatial context. Fig. 1 also

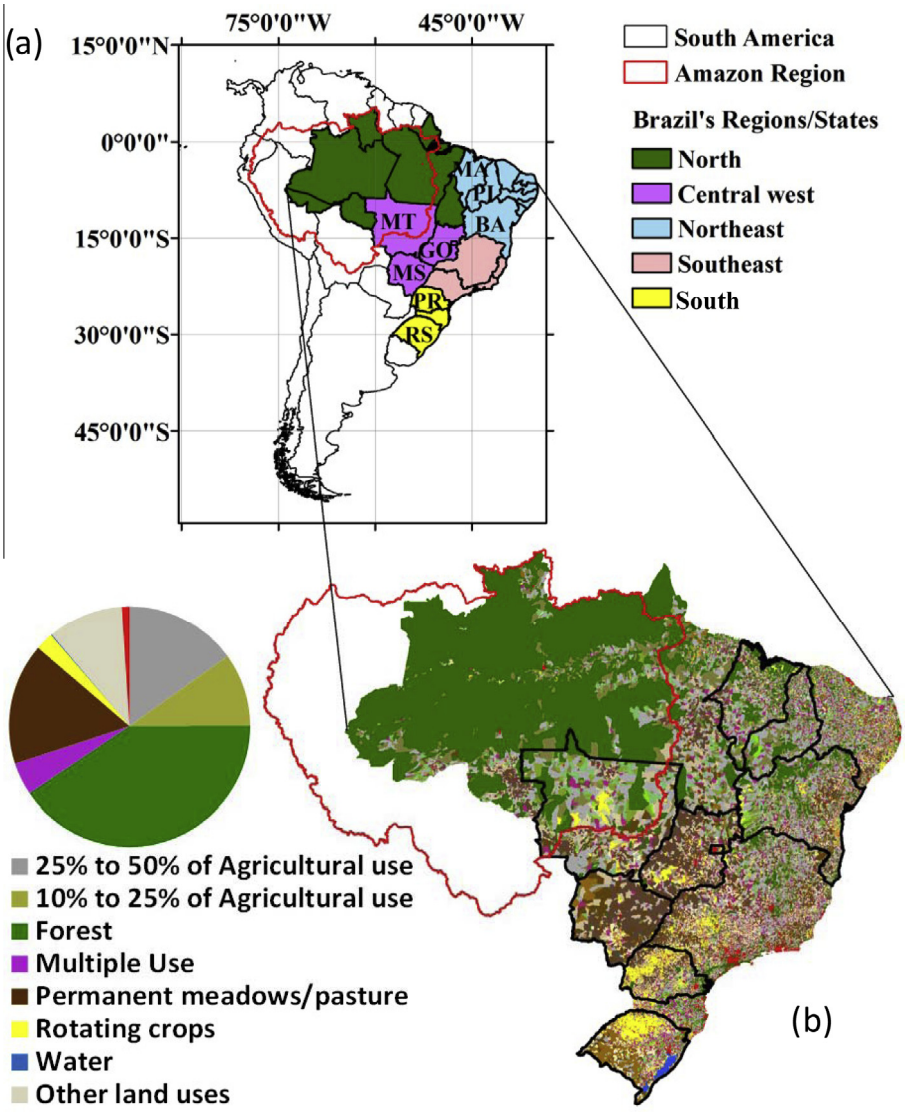

Fig. 1. (a) Study region, highlighting regions/states in Brazil used in correlation analyses. Also shown is (b) a map of land use over Brazil circa 2006 (IBGE, 2010).

highlights generalized geographic regions (South, Northeast, Central West and Amazon) of Brazil that are of interest in the drought analyses, as well as the agricultural states of Maranhão (MA), Piauí (PI), Bahia (BA), Mato Grosso (MT), Mato Grosso do Sul (MS), Goiás (GO), Paraná (PR), and Rio Grande do Sul (RS) in which correlations between drought indicators are assessed (see Table 1).

Landuse in the country of Brazil is shown in Fig. 1b. This map is based on the last agricultural census carried out in 2006 by the Brazilian Institute of Geography and Statistics (IBGE; http://www.ibge.gov.br/english/) and demonstrates the prevalence of forest over north Brazil (principally Amazonia), and the transition into partial to predominant agricultural use toward the south and east. Crops grown in rotation (primarily soybean, corn and wheat) are found predominantly in the south and southeast, but are expanding north with new fronts of land occupation. The central-west region is dominated by cultivated pasture, which has been replacing natural pasture since 1985. The largest area of extractive agriculture is in the north, while the northeast region is distinguished by a great diversity of agricultural and extractive uses.

3. Remote sensing data

3.1. Leaf area index

To evaluate drought impacts on green vegetation amount, daily LAI maps over the South American domain were obtained from the 4-day global 1-km MODIS LAI product (MCD15A3 Terra-Aqua combined, Collection 5), available from mid-2002 to present. The product was temporally smoothed and gap-filled following the procedure described by Gao et al. (2008), based on the TIMESAT algorithm of Jonsson and Eklundh (2004). In this procedure, an adaptive Savitsky-Golay smoothing filter is applied to the LAI time-series at each pixel, with weighting factors set based on retrieval quality. In specific, two quality control (QC) layers (FparLai_QC and FparExtra_QC) in the MODIS LAI product are interrogated to ensure clear and high quality retrievals receive higher weights. If sufficient high quality retrievals are not available during some time period, an appropriate land-cover class dependent seasonal curve is identified among neighboring pixels with good annual coverage and adjusted based on the available timeseries data. The fit curve is used to fill gaps during persistently cloudy

Table 1
States and regions considered in the timeseries and correlation analyses. Also given are regionally averaged temporal correlation coefficient $\langle r \rangle$ computed between f_{RET}, LAI and TRMM timeseries and anomaly timeseries (all 1-month composites).

Acronym	State/region	Region	Correlations					
			f_{RET} v. TRMM	f_{RET} v. LAI	LAI v. TRMM	ESI v. TRMM′	ESI v. LAI′	LAI′ v. TRMM′
AM	Amazon	North	0.43	−0.16	−0.21	0.20	−0.04	−0.09
MA	Maranhão	Northeast	0.66	0.78	0.35	0.19	0.37	0.03
PI	Piauí		0.69	0.84	0.61	0.19	0.45	0.06
BA	Bahia		0.43	0.70	0.48	0.29	0.57	0.19
MT	Mato Grosso	Central west	0.71	0.58	0.47	0.39	0.29	0.16
MS	Mato Grosso do Sul		0.52	0.81	0.51	0.46	0.47	0.26
GO	Goiás		0.76	0.92	0.78	0.50	0.52	0.31
PR	Paraná	South	0.38	0.68	0.19	0.54	0.46	0.27
RS	Rio Grande do Sul		0.16	0.46	0.05	0.27	0.39	0.21

intervals. This procedure is implemented to provide full daily timeseries while attempting to minimize the influence of data collected under cloudy conditions or high aerosol loads associated with biomass burning, which are suspected to result in artifacts in time behavior of VI and LAI products over the Amazon (Samanta et al., 2010b).

3.2. Evaporative stress index (ESI)

The ESI represents standardized anomalies in a normalized clear-sky ET ratio, $f_{RET} = ET/ET_{ref}$, where ET is actual ET and ET_{ref} is a reference ET scaling flux used to minimize impacts of non-moisture related drivers on ET (e.g., seasonal variations in radiation load). Here we use the FAO-96 Penman–Monteith (FAO PM) reference ET for grass, as described by Allen et al. (1998). Anderson et al. (2013) compared use of several different scaling fluxes over the continental U.S. and found the FAO PM equation provided best agreement with drought classifications in the US Drought Monitor and with soil moisture-based drought indices.

Actual ET estimates used to generate the ESI products for this study were obtained from a MODIS-based version of the TIR remote sensing Atmosphere-Land Exchange Inverse (ALEXI) model (Anderson et al., 1997, 2007b; Mecikalski et al., 1999). ALEXI uses measurements of the morning surface radiometric temperature rise, typically provided by geostationary satellites (ΔT_{RAD}_GEO), as the main diagnostic input to a two-source (soil + vegetation) model of surface energy balance, effectively based on the principle that wetter surfaces warm less rapidly during the morning hours. Anderson et al. (1997) demonstrated that use of a time-differential LST signal reduces model sensitivity to errors in the absolute temperature retrieval due to errors in atmospheric and emissivity corrections. ALEXI flux estimates have been evaluated over several flux measurement sites across the U.S. and in Europe using a spatial disaggregation technique (DisALEXI; Anderson et al., 2004; Norman et al., 2003), indicating errors in daily actual ET on the order of 10–15% over a broad range in vegetation and climate conditions (Anderson et al., 2012b, 2007a, 2005; Cammalleri et al., 2012, 2013, 2014). For global applications, however, dependence on multiple international geostationary datasets, with differing sensor characteristics, calibrations and temporal extent, is a limiting factor for ALEXI. Therefore, this study employs an analog system that uses polar orbiting MODIS day-night LST observations to derive a proxy for ΔT_{RAD}_GEO (called ΔT_{RAD}_POLAR) through multi-variable regression. MODIS-based values of ΔT_{RAD}_POLAR were evaluated against ΔT_{RAD}_GEO measurements from the Geostationary Operational Environmental Satellites (GOES, U.S.) and Meteosat Second Generation (MSG, Europe) over a six-year study period (2007–2012). This six-year validation period was withheld from the training of the regression algorithm. In general, strong agreement between ΔT_{RAD}_POLAR and ΔT_{RAD}_GEO was found ($R^2 = 0.91$) with root-mean squared errors on the order of 8–10% over the six validation years. The MODIS-enabled ALEXI (ALEXI_POLAR) has the advantage of providing global coverage using a single polar-orbiting platform.

ALEXI_POLAR was executed daily over South America on the 0.1° grid shown in Fig. 1. The model was forced with meteorological inputs from NASA's Modern-Era Retrospective Analysis for Research and Applications (MERRA; Rienecker et al., 2011), ΔT_{RAD} inputs from the MODIS Aqua MYD11C1 climate modeling grid (CMG) product (Collection 5), and LAI from the filtered MODIS product described in Section 3.1. MERRA meteorological data were also used to compute ET_{ref} using the FAO PM approach. Standardized anomaly computations for transforming time composites of f_{RET} time-series into ESI are described in Section 4.1. The procedure uses f_{RET} values retrieved near local noon under clear-sky conditions. It is hypothesized that use of clear-sky ET retrievals (as opposed to all-sky estimates) results in better separation of soil moisture-induced controls on ET from drivers related to variable radiation load such as cloud cover. In addition, thermal retrievals of LST are limited to clear-sky conditions, which poses a challenge in some parts of Brazil during the rainy season.

3.3. Tropical rainfall mapping mission

The TRMM 3B42 v7 precipitation product (Huffman et al., 2007) is used in this study to delineate spatiotemporal variability in moisture supply over the modeling domain. This product is obtained by merging observations acquired at microwave and IR wavelengths. The native product has 0.25° spatial resolution and is provided at daily time-steps. Daily precipitation values over the ALEXI grid were obtained from the closest native TRMM 3B42 pixel.

4. Methods

4.1. Temporal composite and anomaly computations

Standardized anomalies in LAI, TRMM rainfall and clear-sky f_{RET} (i.e., ESI) were computed from temporal composites generated within 4, 8 and 12-week (approximately 1, 2 and 3-month) moving windows advancing at 7-day timesteps. Composites were computed as an unweighted average of all index values over the interval in question:

$$\langle v(w,y,i,j)\rangle = \frac{1}{nc}\sum_{n=1}^{nc} v(n,y,i,j), \quad (1)$$

where v represents LAI, rainfall or f_{RET}, $\langle v(w,y,i,j)\rangle$ is the composite for week w, year y, and i, j grid location, $v(n,y,i,j)$ is the value on day n, and nc is the number of days with good data during the

compositing interval. Cloudy-day values from ALEXI_MODIS were flagged and excluded from the composites. To avoid composites computed from only a few unflagged values during pervasively cloudy periods, a threshold of 50% of total days within the window had to be exceeded or the ESI composite pixel was flagged as bad. This leads to missing data in ESI over the Amazon during the rainy season, particularly between December and February. The TRMM and MODIS LAI datasets were completely filled and therefore exhibit no blanking due to data gaps.

All composited indices were then transformed into a "z-score", normalized to a mean of zero and a standard deviation of one. Fields describing "normal" (mean) conditions and temporal standard deviations at each pixel are generated for each compositing interval over the baseline period 2003–2013. Then standardized anomalies at pixel i, j for week w and year y are computed as

$$v(w,y,i,j)' = \frac{\langle v(w,y,i,j)\rangle - \frac{1}{ny}\sum_{y=1}^{ny}\langle v(w,y,i,j)\rangle}{\sigma(w,i,j)}, \quad (2)$$

where the second term in the numerator defines the normal field, averaged over all years ny, and the denominator is the standard deviation. In this notation, f_{RET}' computed for an X-month composite is referred to as ESI-X, where X is 1, 2 or 3. A range of composite intervals is useful for investigation of drought impacts at different timescales (e.g., discriminating between meteorological and agricultural drought). Furthermore, longer timescale composites in ESI and ET will have more complete coverage over the modeling domain during the rainy season. For example, the average missing data fraction over the Amazon region (Fig. 1) peaks in late March at about 60% in ESI-1, 30% in ESI-2 and 20% in ESI-3. In comparison, during the dry season the missing data fractions over this region average around 2%, 1% and 0.5% for ESI-1, -2, and -3, respectively. In addition, longer term dry-season anomalies for May to October were computed to summarize annual variability in each index.

5. Results

5.1. Climatological patterns

The August-October composite of clear-sky midday latent heat flux in Fig. 2, generated with ALEXI_POLAR for 2013, illustrates the strong north–south gradient in evaporative flux that exists across the South American continent. The MODIS LST inputs to ALEXI_POLAR capture details in the hydrologic landscape, including enhanced evaporative flux over the Amazon River network in Brazil and the Paraná River extending into Argentina. Similar ET enhancements have been identified in ALEXI ET products over major river networks in the U.S. (Hain et al., 2015) and in the Nile basin (Yilmaz et al., 2014). In addition, reductions in ET associated with major forest logging cuts in the northern Brazilian state of Pará are evident in Fig. 2. ET is depressed relative to normal over northeast Brazil in this year due to a persistent severe drought that started in 2012.

The seasonal cycles in precipitation, reference ET ratio (f_{RET}) and MODIS LAI, and cross-correlations between these variables, are also highly variable over this geographic domain. Annual timeseries of clear-sky f_{RET}, averaged over the baseline period

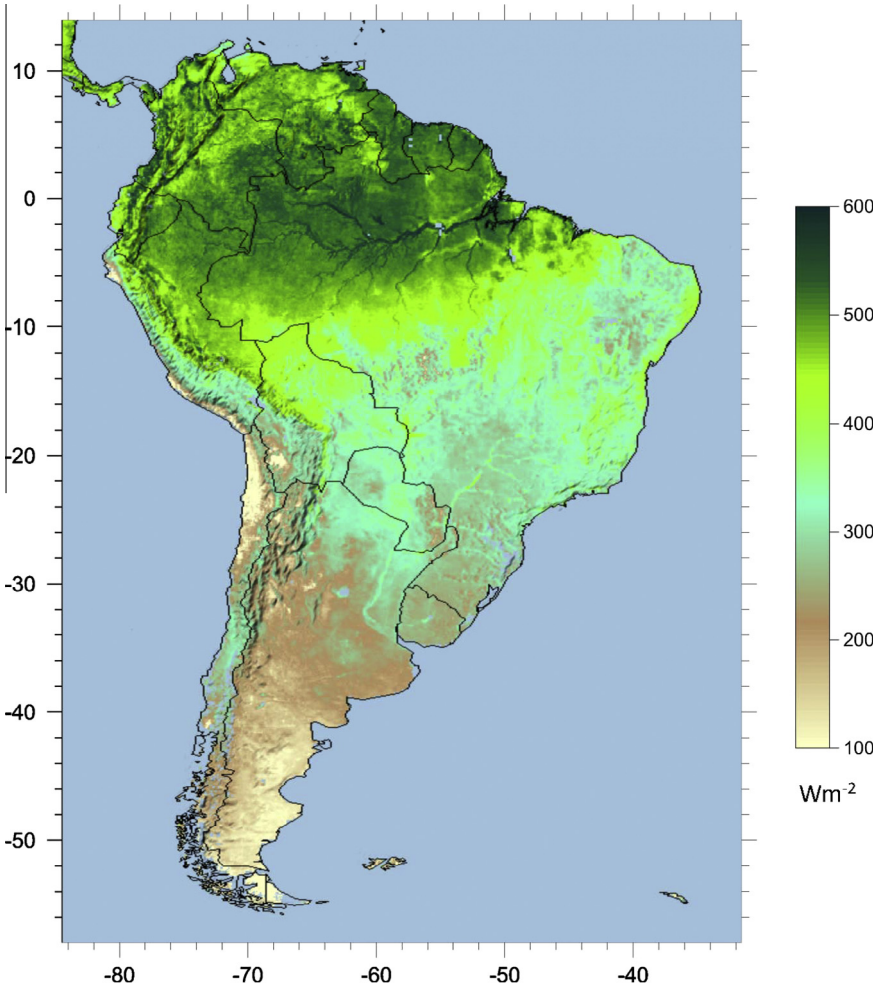

Fig. 2. August–October composite of clear-sky midday latent heat flux for 2013.

2003–2013 and over the selected Brazilian states/regions in Table 1, are compared with climatological MODIS LAI and TRMM precipitation cycles in Fig. 3. Fig. 4 presents maps of temporal cross-correlation between f_{RET}, TRMM, MODIS LAI products sampled at monthly intervals throughout the 11-year timeseries, with region-averaged correlation statistics summarized in Table 1. In computing these correlations, LAI and TRMM timeseries were flagged using the ESI product to ensure consistent temporal sampling between product pairs during the rainy season. The products were composited to1-month intervals to reduce temporal dependence between data samples.

The Amazon region, along with forested areas of Chile and Argentina, show significant anticorrelation between the filtered/smoothed MODIS LAI and the TRMM and f_{RET} timeseries, with average correlation coefficient ($\langle r \rangle$) of −0.21 and −0.16, respectively (Fig. 4; Table 1). Normal timeseries averaged over the Amazon basin show a modest peak in MODIS LAI during the dry season (May through October), with annual variation between 4.4 and 5.2 (Fig. 3). This is consistent with the findings of Myneni et al. (2007) for the period 2000–2005, who argued that the seasonal cycle in LAI in the Amazon is primarily driven by the annual insolation curve, with flushing of new leaves occurring near the beginning of the dry season and abscission beginning with the onset of the rainy season – i.e., out of phase with the rainfall cycle. This interpretation, however, is inconsistent with in situ measurements of LAI inferred from canopy light interceptance and tower measurements of gross ecosystem exchange of carbon dioxide, both of which show a minimum during the dry season (Doughty

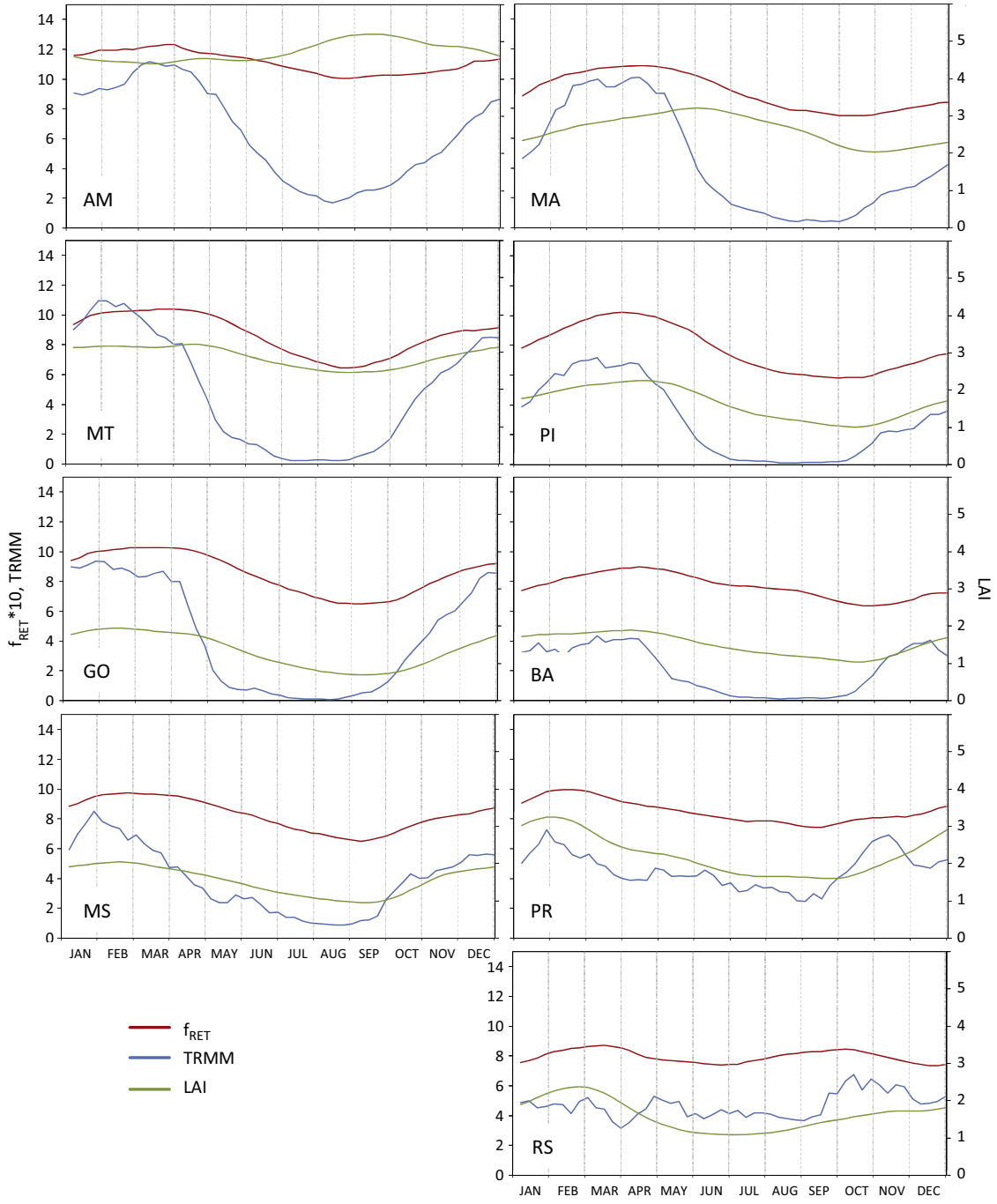

Fig. 3. Multi-year (2003–2013) normal curves for fRET [–], TRMM precipitation [mm $d-1$] and MODIS LAI [–] averaged over the regional polygons defined in Fig. 1.

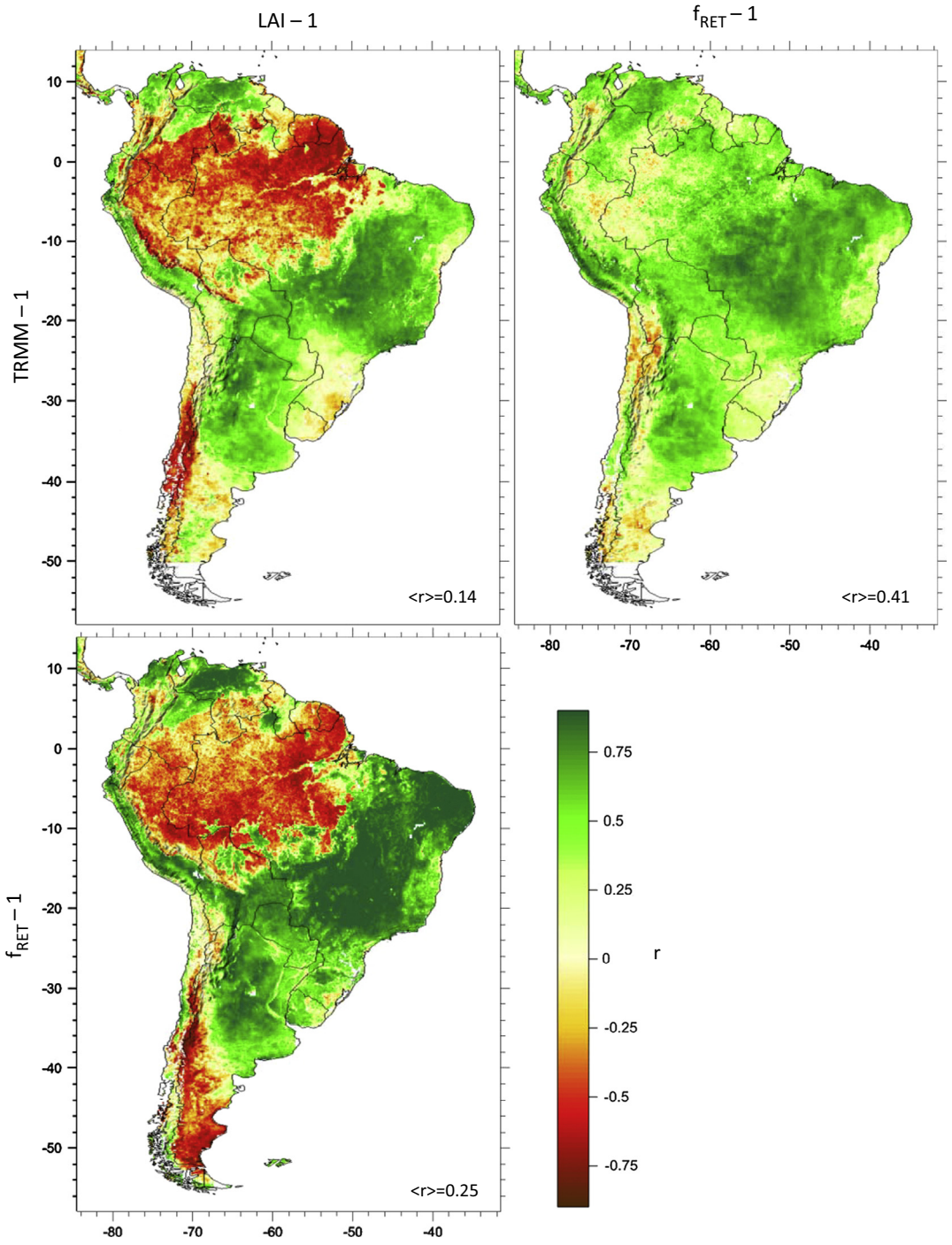

Fig. 4. Cross-correlation between 11 year timeseries of 1-month composites of f_{RET}, TRMM precipitation and MODIS LAI sampled at monthly intervals.

and Goulden, 2008). Doughty and Goulden hypothesize the apparent increase in LAI from the MODIS retrieval algorithm is related to spectral properties of new green leaves generated during the dry season flush, which tend to have higher reflectances in the NIR than older leaves, rather than an actual increase in biomass. Therefore, areas of strong anticorrelation with LAI in Fig. 4 may be due in part to spectral artifacts and require further investigation.

In contrast, the f_{RET} timeseries are positively correlated with TRMM precipitation rates over most of the continent, with $\langle r \rangle = 0.43$ over the Amazon and higher correlations in areas dominated by savanna, grasslands, crops and pasture (Fig. 4; Table 1). TRMM and MODIS LAI correlations are also predominantly positive over non-forested landcover classes. Correlations of both f_{RET} and LAI with TRMM are reduced in the southern states of Paraná and particularly Rio Grande do Sul in comparison with more northern states (Fig. 4; Table 1) because the amplitude of the average seasonal rainfall pattern is relatively weak in the south (Fig. 3). A similar degradation in correlations related to depressed seasonal rainfall amplitude is observed in parts of eastern Brazil, including the coastal region of Bahia.

5.2. Anomalies

While the climatological assessments in Section 3.2 reveal seasonal tendencies in satellite retrievals of rainfall, biomass, and evapotranspiration, analyses of anomalies from the seasonal norms

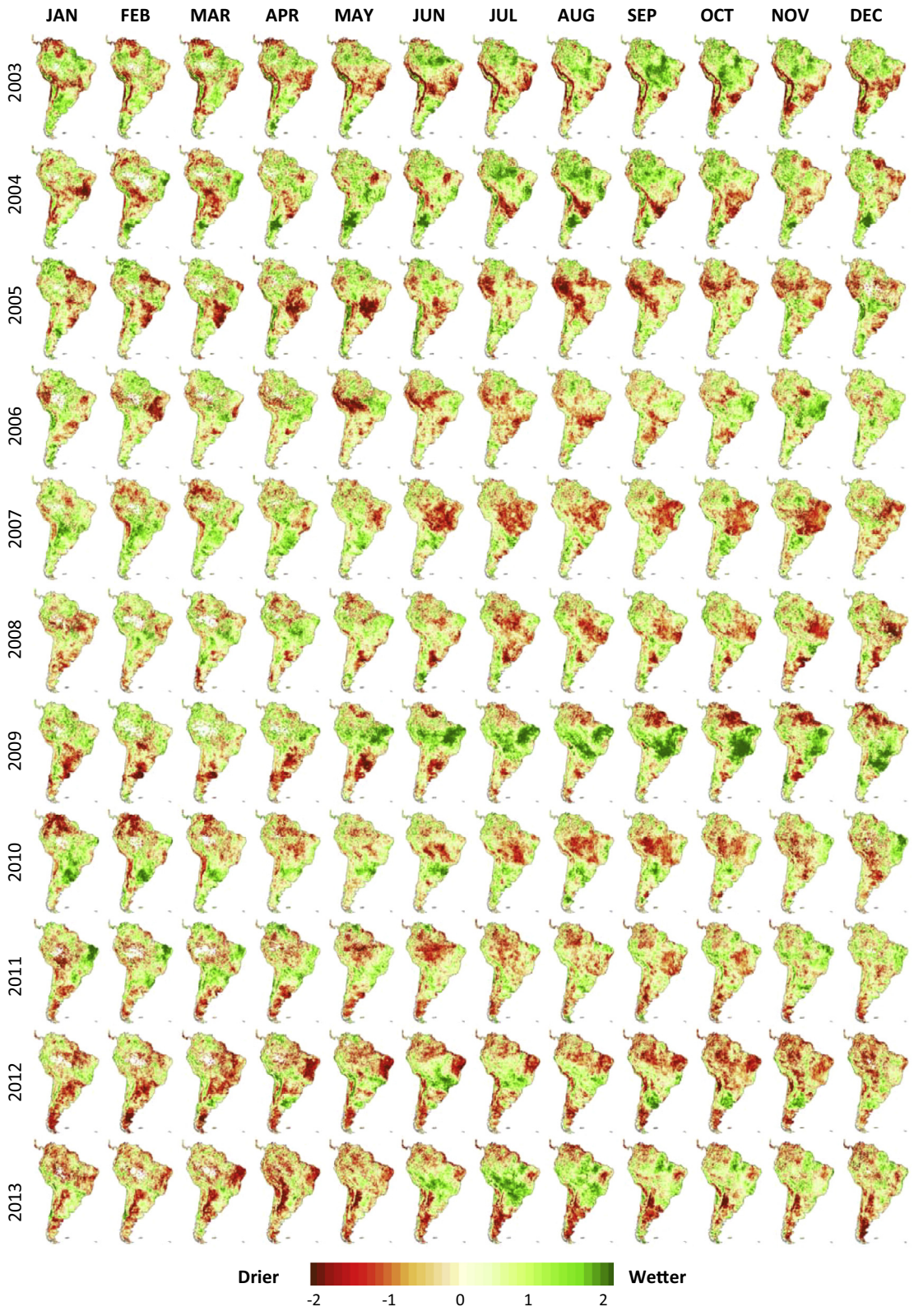

Fig. 5. Monthly maps of ESI-2 for 2003–2013.

focus on how these quantities co-vary in response to year-to-year variability in weather and moisture conditions, as well other potential stressors.

Monthly maps of ESI-2 for 2003–2013 in Fig. 5 describe the cycle of drought and pluvial patterns observed over the South American continent during the past decade as evidenced in the evaporative loss component of the hydrologic budget. Here, 2-month composites are used to improve spatial coverage during the rainy months while retaining month-to-month variability. Major Amazon droughts in 2005 and 2010 are captured by the

ESI, as well as a flood event of 2009 (Marengo et al., 2008, 2011, 2013b). The persistent drought from 2012 to 2013 in the northeast states is also apparent.

Compared on an annual timestep in Fig. 6, maps of ESI, TRMM and MODIS LAI dry season anomalies (composited from May to October, where ESI coverage is fairly complete) generally exhibit similar spatial patterns. Exceptions include strong departures of LAI anomalies during the 2005 drought and 2009 flood events over the Amazon (Fig. 6). These events are discussed further below.

Maps of temporal correlations between ESI-1 and anomalies in 1-month composites of TRMM precipitation and LAI, each sampled at monthly intervals, are shown in Fig 7. Again, TRMM and LAI timeseries were flagged consistent with the ESI-1 timeseries to ensure comparable temporal sampling over the central Amazon. In these plots, correlations $|r| > 0.18$ are significant at $p < 0.05$. As with the seasonal LAI timeseries in Fig. 4, an anticorrelation with anomalies in LAI is observed over the Amazon rainforest, whereas significant positive correlations between ESI and TRMM′ and LAI′ are observed in grassland and agricultural areas characterized by shorter vegetation.

In the sections that follow, the spatiotemporal behavior of the ESI, TRMM and LAI anomaly products as exemplified in Figs. 5–7 are examined in greater detail, with specific focus on the Amazon and agricultural production regions of Brazil.

5.2.1. Regional anomalies over the Amazon

In Fig. 8, timeseries of monthly ESI, TRMM and LAI standardized anomalies for 2003–2013, area-averaged over the Amazon basin, clearly demonstrate the anticorrelation that exists in this region between MODIS LAI anomalies and the moisture-related drought indicators (Fig 7). Here, 3-month composites have been used to suppress high temporal frequency noise in all products. ESI and TRMM anomalies show stronger temporal correspondence, but there are periods where the correlations break down. Notable departures follow the dry season droughts of 2005 and 2010, where negative anomalies in ESI persist several months after precipitation anomalies start to improve, as indicated in the ESI – TRMM′ anomaly differences plotted in Fig. 8. This delayed equilibration behavior suggests memory of antecedent precipitation deficits associated with the deep rootzone soil moisture pool that supports transpiration fluxes in this densely forested region. In contrast, positive rainfall anomalies during the dry seasons in both 2003 and 2004 preceded ESI enhancements that persisted throughout 2004 and into the 2005 drought (Fig. 8). This persistent elevation in reference ET fraction contributes to differences between May-Oct ESI and TRMM anomalies for 2004 observed in Fig. 6.

July–September (JAS) anomalies in LAI, f_{RET} and TRMM precipitation associated with the 2005 and 2010 Amazon droughts and May–July (MJJ) anomalies during the 2009 flood are shown in Fig. 9, demonstrating varying degrees of agreement between these three indicators as discussed below.

2005 Drought: Both TRMM′ and ESI capture the drought event of 2005 (Fig. 9), which began around April of that year and strongly affected western Amazonia, over an area comprising the state of Acre and part of Amazonas, as well as some parts of border countries (Marengo et al., 2008). In contrast, LAI anomalies peak at positive values in early August, a few weeks before the negative minima in the ESI and TRMM anomaly timeseries (Fig. 8). A similar temporal anticorrelation was observed by Anderson et al. (2010), comparing MODIS EVI (C5) and TRMM rainfall anomalies for 2005 over the Amazon. Patterns of positive MODIS LAI anomalies for the July–September period of 2005 (Fig. 9) resemble those in the cloud and aerosol screened EVI maps in Samanta et al. (2010a), both in spatial distribution and anomaly magnitude. Saleska et al. (2007) found even stronger positive EVI anomalies with the MODIS C4 version and attributed this to drought-induced green-up in an energy limited vegetation system due to decreased cloudiness – a claim that has been challenged in other studies as an artifact of incomplete screening of poor quality data (Samanta et al., 2010a, 2010b). In addition, Phillips et al. (2009) observed widespread dieback in Amazon monitoring plots following the 2005 drought, in apparent contradiction with the drought green-up hypothesis, but more consistent with the vegetation stress patterns identified by the ESI (Fig. 9). While the Timesat-processed MODIS LAI timeseries used here also show a small positive increase on average over the Amazon basin during the 2005 drought, f_{RET} anomalies suggest a strong decrease in vegetation water use during JAS, particularly over the western region where precipitation deficits were strongest. Given that water loss is predominantly through transpiration during this period, this would imply a decrease in canopy conductance and photosynthetic activity, consistent with tower water and carbon flux observations in southwestern Amazonia (Zeri et al., 2014).

2010 Drought: Strong negative ESI and TRMM anomalies are also evidenced during the 2010 Amazon drought in central West Brazil,

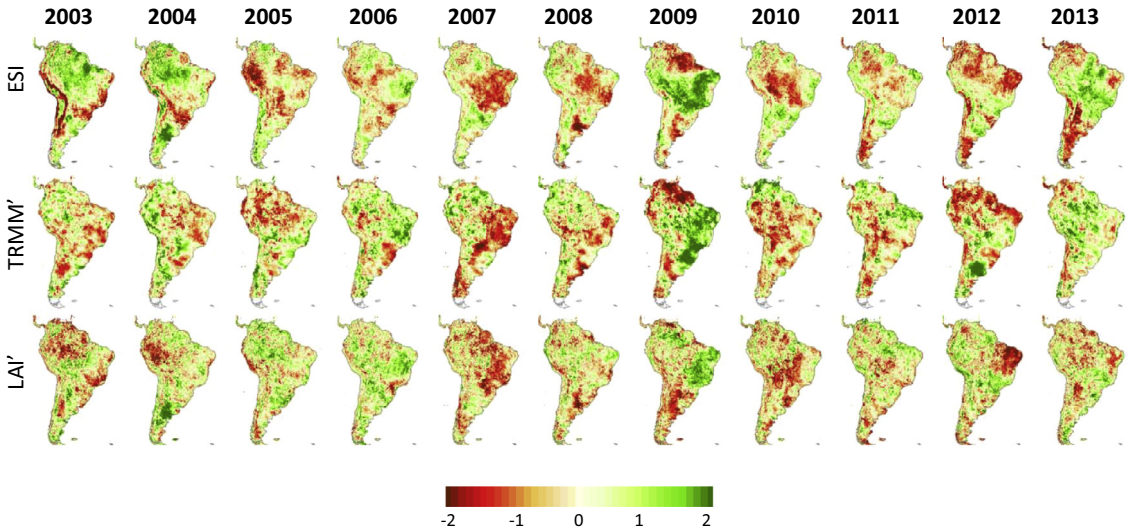

Fig. 6. Annual standardized anomalies in f_{RET} (ESI), TRMM precipitation and MODIS LAI (May to October composites) for 2003–2013.

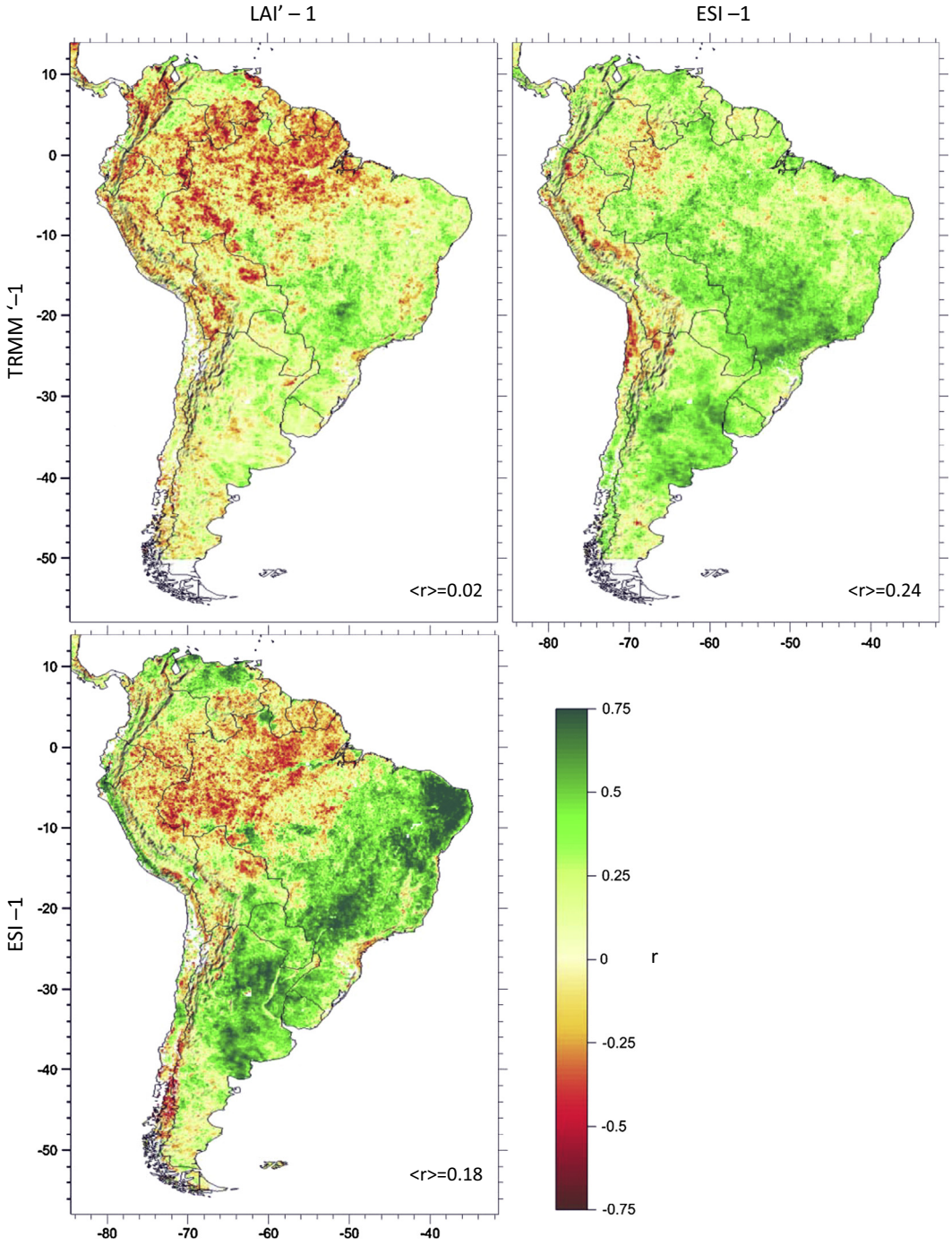

Fig. 7. Cross-correlation between 11 year timeseries of 1-month composites of f_{RET}, TRMM precipitation and MODIS LAI standardized anomalies sampled at monthly intervals.

comprising part of the state of Mato Grosso and spreading to southwestern Amazonia and border countries from July through September/October (Figs. 5 and 9). In this case, LAI′ also showed a response during the dry season, turning negative after July (Fig. 8) with area of impact similar to that seen in the ESI JAS anomalies (Fig. 9). The LAI anomalies in Fig. 9 resemble spatial patterns in JAS MODIS EVI (C5) anomalies for 2005 and 2010 published by Xu et al. (2011), comparing magnitude and spatial extent of greenness declines between these two Amazon dry season drought events. Based on negative anomalies in EVI and NDVI products subjected to rigorous cloud and aerosol clearing, Xu et al. (2011) conclude that the 2010 drought impacted a larger percentage area of rainforest than did 2005 (51.4% vs. 14.3%), in general agreement with comparisons by Lewis et al. (2011) using TRMM data. According to Fig. 9, the water use impacts in 2005 were disproportionately large in comparison with apparent greenness declines, while impacts were more comparable in the 2010 drought.

2009 Flood: In contrast, during 2009 heavy rainfall in northeast Brazil began in early April and persisted for several months, causing a major flood event which devastated several states in the region, as was widely reported by national and international media. During this year, the water level of the Rio Negro recorded at Manaus reached 29.77 m, representing a return interval of

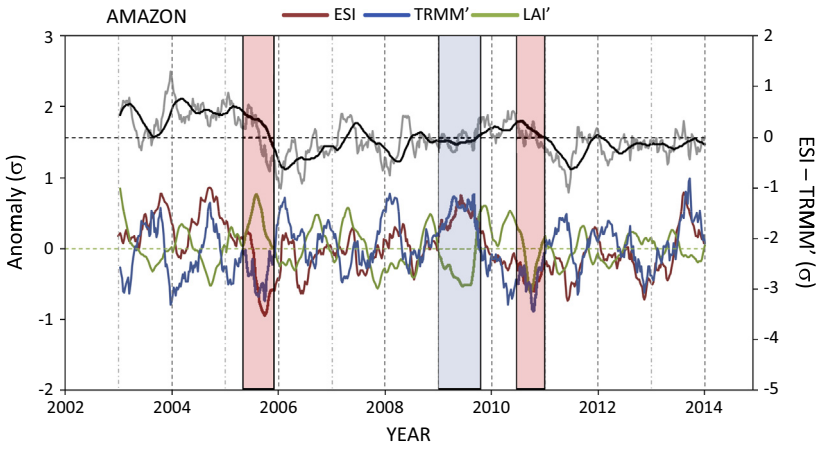

Fig. 8. Eleven year timeseries of f_{RET}, TRMM precipitation and MODIS LAI standardized anomalies (3-month composites) sampled at weekly intervals and averaged over the Amazon basin (AM in Fig. 1). Major Amazon droughts of 2005 and 2010 are highlighted with red boxes, and the pluvial of 2009 in blue. Also shown are differences between ESI-3 and TRMM′-3 (gray line), with a 20-week moving average superimposed (black line). (For interpretation of the references to colour in this figure legend, the reader is referred to the web version of this article.)

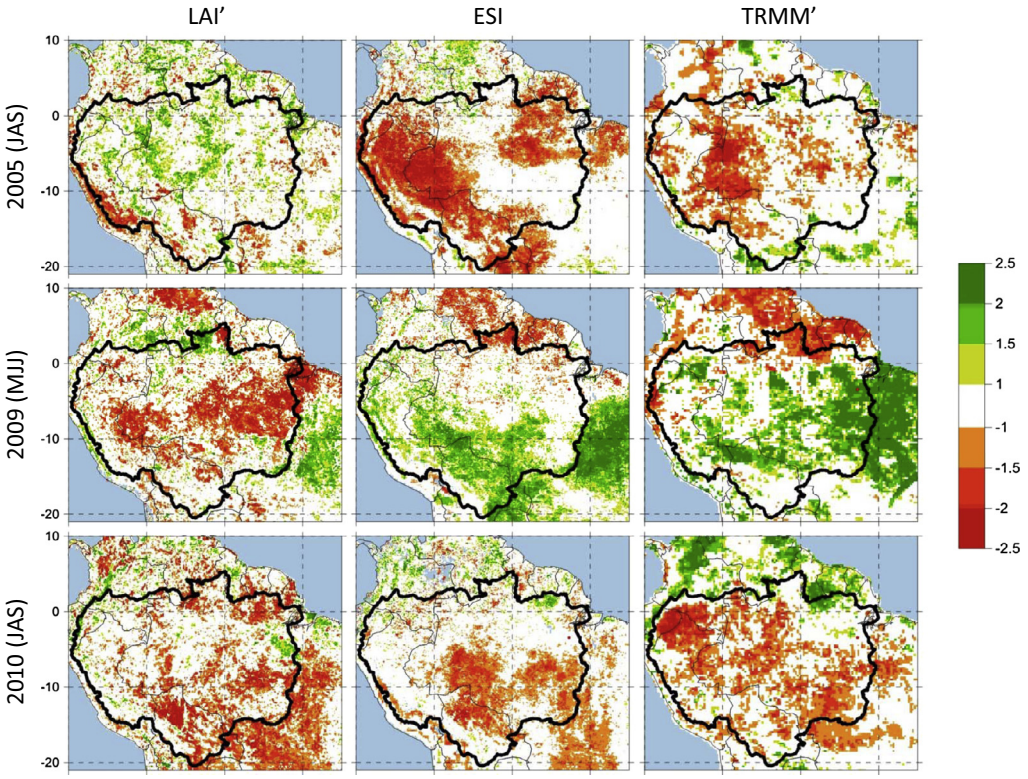

Fig. 9. JAS standardized anomalies in LAI, f_{RET} (ESI), and TRMM for 2005 (top row) and 2010 (bottom row), and MJJ anomalies for 2009 (middle row). The Amazon basin is outlined in black.

55 years. This pluvial is also evident in Figs. 6 and 9, with well-correlated positive ESI and TRMM anomalies peaking midyear (Fig. 6). Spatiotemporal patterns in the ESI and precipitation anomalies from TRMM satellite in Figs. 5 and 6 agree well with those presented in Marengo et al. (2012). Monthly evolution in positive ESI through 2009 (Fig. 5) also shows some spatial correspondence with regions of significant increase in terrestrial water storage (TWS) diagnosed by Chen et al. (2010) using the Gravity Recovery and Climate Experiment (GRACE). LAI anomalies, however, are strongly anticorrelated with ESI and TRMM′ during this time period (Fig. 8). Peak negative LAI anomalies (of magnitude on the order of −0.3 to −0.7 in LAI units) occur from May to July in a band spatially coincident with areas of highest TRMM precipitation (Fig. 9). Areas of anomalous "browning" in 2009 were also noted by (Samanta et al., 2012) in an analysis of 2000–2009 MODIS EVI timeseries.

5.2.2. Regional anomalies over agricultural production areas

Timeseries of ESI, TRMM and LAI anomalies for the 8 Brazilian agricultural states listed in Table 1 are shown in Fig. 10, along with plots of ESI – TRMM′ departures. In contrast to the Amazon basin, the ESI, TRMM and LAI anomalies over these regions with

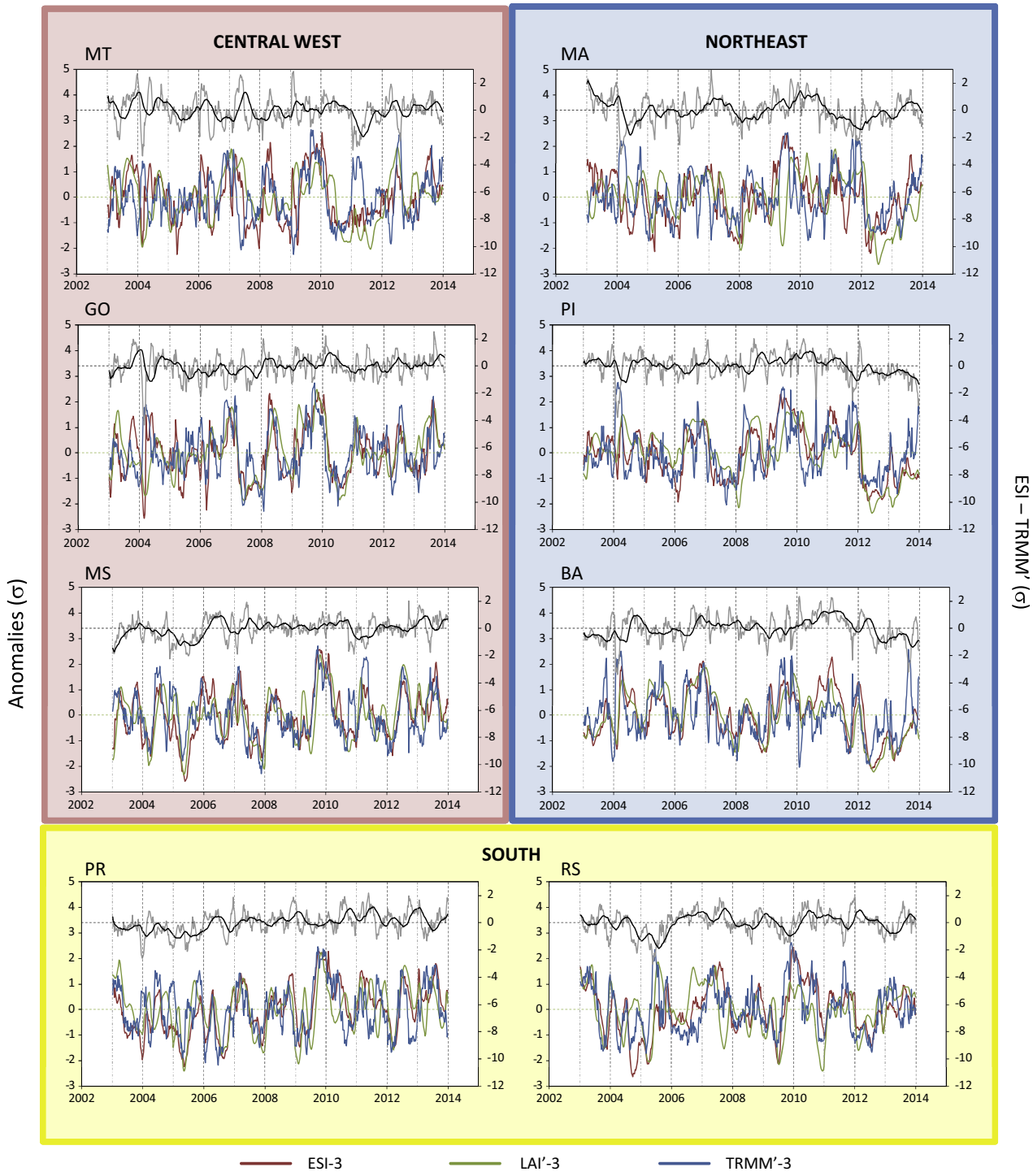

Fig. 10. Eleven year timeseries of f_{RET}, TRMM precipitation and MODIS LAI standardized anomalies (3-month composites) sampled at weekly intervals and averaged over agricultural regions in the 8 Brazilian states listed in Table 1. Also shown are differences between ESI-3 and TRMM′-3 (gray line), with a 20-week moving average superimposed (black line).

predominantly short vegetation show reasonable agreement, lacking the strong anticorrelation with LAI evident in Fig. 8. ESI – TRMM′ departures for most of these states do not exhibit the same degree of temporal coherence observed for the Amazon. An exception is in Mato Grosso (MT), where the response to the 2010 drought resembles that observed in AM. This drought encompassed MT, which abuts the Amazon basin and still includes patches of uncleared forest. A few hydrologic extreme events are evident across most geographic regions and indicators in Fig. 10 – most prominently the pluvial of 2009, and a widespread drought afflicting eastern Brazil in 2007 (Fig. 5). In addition, several regional droughts have caused great losses for the agricultural sector during the last decade.

For example, the southern region of Brazil (including PR and RS) experienced severe "flash" drought events during 2005, 2009 and 2012, significantly impacting crop yields (FARSUL, 2013; Sousa Junior et al., 2012). A comparison of ESI with LAI and TRMM anomalies over south and northeast Brazil during

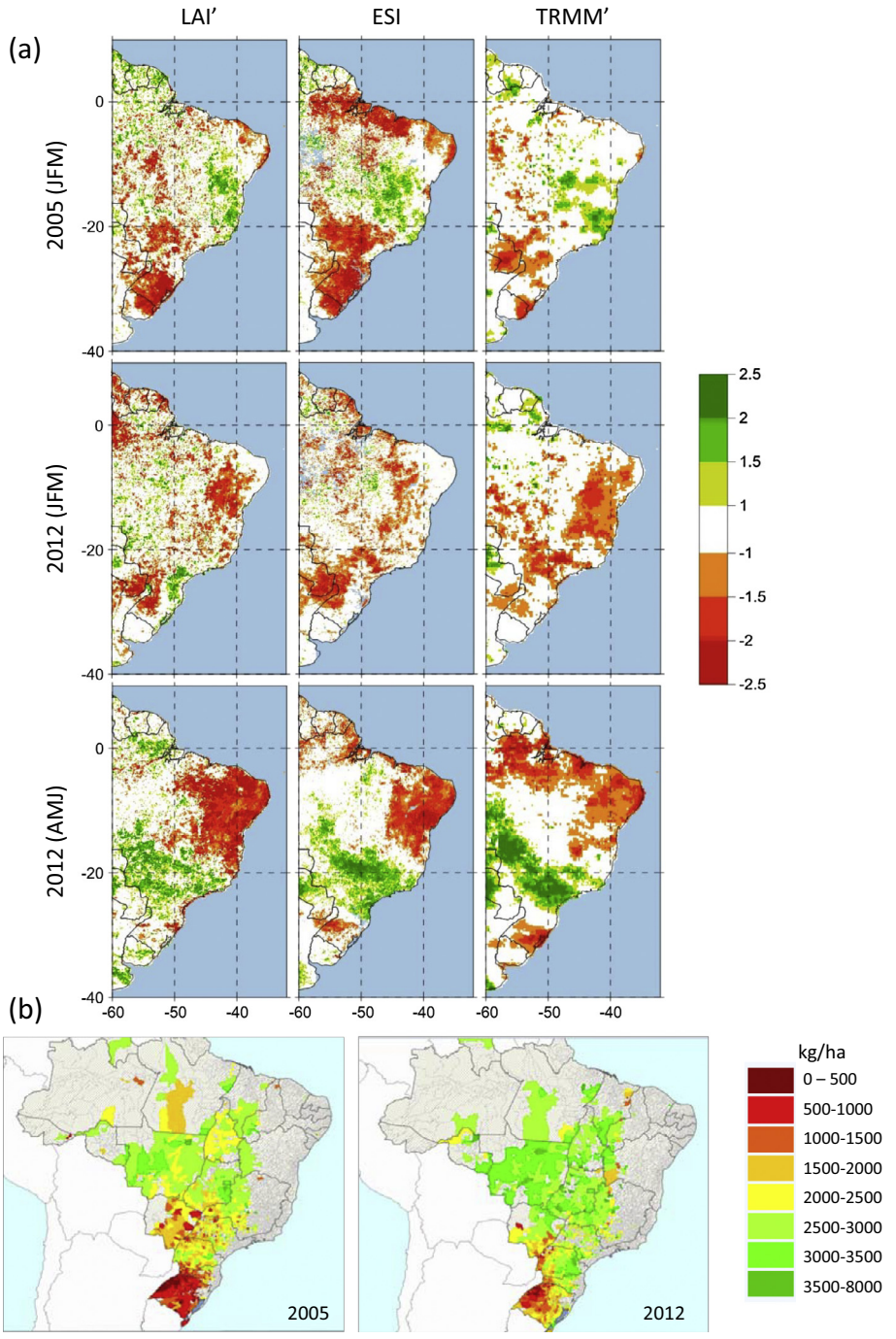

Fig. 11. (a) Standardized anomalies in LAI, f_{RET} (ESI), and TRMM for JFM 2005 (top row), JFM 2012 (middle row), and AMJ 2012 (bottom row). (b) Municipal level soybean yield maps for the 2005 and 2012 harvests (IBGE).

austral summer (January to March, JFM) for 2005 and 2012 (Fig. 11) show good agreement between indicators, and with MODIS EVI anomalies published by Sousa Junior et al. (2012). This is a period of maximal sensitivity of regional soybean crops (typically planted in November and harvested in March) to soil moisture deficits. Municipalities with reduced soybean yield harvested in 2005 and 2012, as reported by IBGE, coincide with areas of anomalously low precipitation, LAI, and reference ET ratio during JFM, indicating degraded vegetation health and moisture availability (Fig. 11).

Starting in April 2012, the epicenter of drought in Brazil shifted to the northeast, where it persisted throughout the year and into 2013 (Fig. 5). Gutiérrez et al. (2014) report that the 2012–2013 northeast drought has been one of the most severe in 100 years, with many municipalities declaring a state of emergency and yield losses in rainfed agricultural systems on the order of 90% compared to 2011. LAI′, TRMM′ and ESI show similar patterns of drought signal migration between JFM and AMJ (Fig. 11). Again, this is in contrast with the typical behavior observed over the Amazon where the signals from these indicators are often highly decoupled during periods of rapid change in hydrologic status. This suggests stronger control by precipitation deficits on biophysical functioning (water use and biomass production) in these agricultural ecosystems in comparison with the evergreen forests of the Amazon, where deeper rooting systems may induce time lags between patterns of water supply and consumption.

6. Discussion

Comparisons between ESI, MODIS LAI and TRMM precipitation timeseries for the period 2003–2013 suggest that LAI and TIR-based relative ET anomalies over the Amazon give a very different picture of biosystem response to hydrologic extremes. This may be due to in part to residual cloud and aerosol contamination in the MODIS LAI C5 products, or to biophysical issues such as changes in leaf spectral properties with age. The difference in response may also reflect cumulative physical impacts resulting from rapidly recurring hydrological extremes. We note that Collection 6 MODIS reprocessing is underway, and enhanced aerosol and atmospheric corrections or changes to the LAI algorithm in C6 may alter the trends and findings reported here.

Toomey et al. (2011) note that in the face of such conflicting evidence, an independent measure of biophysical stress is beneficial. They evaluated day and nighttime MODIS LST anomalies as an independent indicator of stress and found evidence that heat stress played a role in tree mortality observed during the 2005 and 2010 Amazon droughts. Here, morning surface temperature rise (ΔT_{RAD}) inferred from day-night MODIS LST temperature differences are interpreted as a diagnostic signal of evaporative flux, predominantly partitioned to transpiration during the dry season over the rainforest. Given the strong coupling between carbon uptake and water loss by transpiration, T_{RAD} and ΔT_{RAD} may also be effective and independent proxy indicators of drought impacts on carbon sinks (Anderson et al., 2008). In the case of the 2005 drought, ESI suggests a more extensive impact on transpiration (and therefore carbon uptake) than indicated by LAI anomalies alone. Impacts are more similarly depicted by the two indicators during the second drought in 2010, which may indicate a stronger sensitivity in biomass production in the face of the recurrent moisture deficits.

While cross-correlations between ESI and TRMM anomalies are stronger than those with LAI′, relative excursions between the two timeseries appear to suggest different timescales associated with water supply and water consumption components of the hydrologic budget within the Amazon basin. The rootzone soil moisture profile may refill more quickly after a severe dry season drought (e.g., 2005 and 2010) than the trees can recover. Similarly, in wetter times, the deep-rooted vegetation may be more resilient to short periods of wet season dry spells (e.g., 2003–2004).

In unforested parts of Brazil, reference ET fraction, precipitation and LAI anomalies show stronger temporal coupling. The moisture capacitance afforded by the shallower rooting systems in these areas is reduced in comparison with that of the rainforest (Nepstad et al., 1994). All three biophysical indicators are well-related to drought impacts as reflected in crop yield variability, at least in the south where crops are more responsive to climate due to a lesser degree of mechanization in comparison with northern corporate cropping systems (Sentelhas et al., 2015). A detailed analysis of yield correlations for different regions, crop types and drought indicators is in progress. For yield estimation, a multi-index approach may prove optimal, given the diversity and range in driving factors and response that exist across the country of Brazil.

While TIR-based retrievals of ΔT_{RAD} from geostationary and polar orbiting satellites provide an independent diagnostic of vegetation stress, sampling in central Amazon is limited during December to March due to persistent cloud cover, inhibiting retrieval of LST using thermal infrared imaging. Incorporation of alternative modes of LST retrieval, for example using passive microwave imaging combined with modeling, into the ESI system is being explored as a means to filling rainy season gaps, particularly problematic in equatorial regions (Holmes et al., 2015). In addition, fusion of higher resolution TIR-based retrievals using Landsat appears a promising approach for evaluating evaporative stress at higher spatial scales (down to 30 m), and for validating ESI and ET retrievals at flux measurement sites – at scales commensurate with the flux tower footprint (Cammalleri et al., 2013, 2014).

7. Conclusions

Time-series of MODIS LAI and TRMM precipitation products for the South American continent and the time period 2003–2013 were compared with a remotely sensed retrieval of actual-to-reference ET ratio (f_{RET}) based on diurnal land-surface temperature changes, with specific focus on relative index behavior over Brazil. Comparisons were conducted both in terms of absolute quantities and standardized anomalies, to separate correlations induced by seasonal patterns from correlations in year-to-year variability associated with drought and pluvial events.

Consistent with prior studies, significant anticorrelation was observed between MODIS LAI and TRMM precipitation values and anomalies over the Amazon rainforest. The cause of this anticorrelation remains ambiguous, and has been ascribed in the literature to either real biophysical responses or artifacts in the LAI retrieval associated with persistent cloudiness and high atmospheric aerosol contents. In contrast, the Evaporative Stress Index (ESI), quantifying standardized anomalies in f_{RET}, shows stronger correlations with TRMM anomalies and minimal anticorrelation over the Amazon region, at variance with claims that the rainforest has greened in response to recent droughts.

Significant positive correlations were observed between LAI, TRMM and ESI timeseries over shorter vegetation classes, including crop and pasture lands. This may reflect stronger coupling between short-term variability in moisture supply (precipitation) and vegetation vigor (ET and LAI) associated with ecosystems with relatively shallow rooting depths, in comparison with the deep-rooted forest systems.

Vulnerability of human populations to exacerbated hydrological extremes is of growing concern in Brazil (Marengo et al., 2013b), leading to increased public discourse regarding strategies for improving drought preparedness and climate resilience in the most susceptible communities (Gutiérrez et al., 2014). Similar discussions are occurring in Sub-Saharan Africa (Zaitchik et al., 2012) and other climate sensitive regions. To best support adaptation measures, a suite of indicators will be necessary – particularly given the ambiguity sometimes conveyed by individual pairs of indicators such as precipitation and LAI. Conversion of ALEXI from a geostationary-based methodology to one using polar orbiting MODIS LST acquisitions facilitates global monitoring of ET and vegetation stress using a single consistent instrument. Prototype global ESI products are currently undergoing initial analyses. Further incorporation of AVHRR LST datasets may provide a means of going back into the 1980s to provide a more complete climate data record of ESI, with continuity provided in the post-MODIS era with the Visible Infrared Imaging Radiometer Suite (VIIRS) on the Joint Polar Satellite System (JPSS) platforms.

Acknowledgments

This research was supported by funding from the Embrapa Visiting Scientist Program and from Labex US, an international scientific cooperation program sponsored by the Brazilian Agricultural Research Corporation – Embrapa, through Contract 10200.10/0215-9 with the Agricultural Research Service – ARS.

all or part of an individual's income is derived from any public assistance program. (Not all prohibited bases apply to all programs.) Persons with disabilities who require alternative means for communication of program information (Braille, large print, audiotape, etc.) should contact USDA's TARGET Center at (202) 720-2600 (voice and TDD). To file a complaint of discrimination, write to USDA, Director, Office of Civil Rights, 1400 Independence Avenue, S.W., Washington, D.C. 20250-9410, or call (800) 795-3272 (voice) or (202) 720-6382 (TDD). USDA is an equal opportunity provider and employer.

References

Allen, R.G., Pereira, L.S., Raes, D., Smith, M., 1998. Crop Evapotranspiration: Guidelines for Computing Crop Water Requirements, United Nations FAO, Irrigation and Drainage Paper 56. Rome, Italy, p. 300.

Anderson, M.C., Norman, J.M., Diak, G.R., Kustas, W.P., Mecikalski, J.R., 1997. A two-source time-integrated model for estimating surface fluxes using thermal infrared remote sensing. Remote Sens. Environ. 60, 195–216.

Anderson, M.C., Norman, J.M., Mecikalski, J.R., Torn, R.D., Kustas, W.P., Basara, J.B., 2004. A multi-scale remote sensing model for disaggregating regional fluxes to micrometeorological scales. J. Hydrometeor. 5, 343–363.

Anderson, M.C., Norman, J.M., Kustas, W.P., Li, F., Prueger, J.H., Mecikalski, J.M., 2005. Effects of vegetation clumping on two-source model estimates of surface energy fluxes from an agricultural landscape during SMACEX. J. Hydrometeorol. 6, 892–909.

Anderson, M.C., Norman, J.M., Mecikalski, J.R., Otkin, J.A., Kustas, W.P., 2007b. A climatological study of evapotranspiration and moisture stress across the continental U.S. based on thermal remote sensing: I. Model formulation. J. Geophys. Res. 112, D10117. http://dx.doi.org/10.1029/2006JD007506.

Anderson, M.C., Kustas, W.P., Norman, J.M., 2007a. Upscaling flux observations from local to continental scales using thermal remote sensing. Agron. J. 99, 240–254.

Anderson, M.C., Norman, J.M., Kustas, W.P., Houborg, R., Starks, P.J., Agam, N., 2008. A thermal-based remote sensing technique for routine mapping of land-surface carbon, water and energy fluxes from field to regional scales. Remote Sens. Environ. 112, 4227–4241.

Anderson, L.O., Malhi, Y., Aragão, L.E.O.C., Ladle, R., Arai, E., Barbier, N., Phillips, O.L., 2010. Remote sensing detection of droughts in Amazonian forest canopies. New Phytol. 187, 733–750.

Anderson, M.C., Hain, C.R., Wardlow, B., Mecikalski, J.R., Kustas, W.P., 2011a. Evaluation of drought indices based on thermal remote sensing of evapotranspiration over the continental U.S. J. Climate 24, 2025–2044.

Anderson, M.C., Kustas, W.P., Norman, J.M., Hain, C.R., Mecikalski, J.R., Schultz, L., Gonzalez-Dugo, M.P., Cammalleri, C., d'Urso, G., Pimstein, A., Gao, F., 2011b. Mapping daily evapotranspiration at field to continental scales using geostationary and polar orbiting satellite imagery. Hydrol. Earth Syst. Sci. 15, 223–239.

Anderson, M.C., Kustas, W.P., Alfieri, J.G., Hain, C.R., Prueger, J.H., Evett, S.R., Colaizzi, P.D., Howell, T.A., Chavez, J.L., 2012b. Mapping daily evapotranspiration at Landsat spatial scales during the BEAREX'08 field campaign. Adv. Water Resour. 50, 162–177.

Anderson, M.C., Allen, R.G., Morse, A., Kustas, W.P., 2012a. Use of Landsat thermal imagery in monitoring evapotranspiration and managing water resources. Remote Sens. Environ. 122, 50–65.

Anderson, M.C., Hain, C.R., Otkin, J.A., Zhan, X., Mo, K.C., Svoboda, M., Wardlow, B., Pimstein, A., 2013. An intercomparison of drought indicators based on thermal remote sensing and NLDAS-2 simulations with U.S. Drought Monitor classifications. J. Hydrometeorol. 14, 1035–1056.

Cammalleri, C., Anderson, M.C., Ciraolo, G., D'Urso, G., Kustas, W.P., La Loggia, G., Minacapilli, M., 2012. Applications of a remote sensing-based two-source energy balance algorithm for mapping surface fluxes without in situ air temperature observations. Remote Sens. Environ. 124, 502–515.

Cammalleri, C., Anderson, M.C., Gao, F., Hain, C.R., Kustas, W.P., 2013. A data fusion approach for mapping daily evapotranspiration at field scale. Water Resour. Res. 49, 1–15. http://dx.doi.org/10.1002/wrcr.20349.

Cammalleri, C., Anderson, M.C., Gao, F., Hain, C.R., Kustas, W.P., 2014. Mapping daily evapotranspiration at field scales over rainfed and irrigated agricultural areas using remote sensing data fusion. Agric. For. Meteorol. 186, 1–11.

Chen, J.-L., Wilson, C.R., Tapley, B.D., 2010. The 2009 exceptional Amazon flood and interannual terrestrial water storage change observed by GRACE. Water Resour. Res. 46, 1–10.

Coelho, C.A.S., Cavalcanti, I.A.F., Costa, S.M.S., Freitas, S.C., Ito, E.R., Luz, G., Santos, A.F., Nobre, C.A., Marengo, J.A., Pezzac, A.B., 2012. Climate diagnostics of three major drought events in the Amazon and illustrations of their seasonal precipitation predictions. Meteorol. Appl. 19, 237–255.

Doughty, C.E., Goulden, M.L., 2008. Seasonal patterns of tropical forest leaf area index and CO_2 exchange. J. Geophys. Res. 113, G00B06. http://dx.doi.org/10.1029/2007JG000590.

Espinoza, J.C., Ronchail, J., Guyot, J.L., Junquas, C., Drapeau, G., Martinez, J.M., Santini, W., Vauchel, P., Lavado, W., Ordoñez, J., Espinoza, R., 2012. From drought to flooding: understanding the abrupt 2010–11 hydrological annual cycle in the Amazonas River and tributaries. Environ. Res. Lett. 7, 1–7.

FARSUL, 2013. Federação da Agricultura do Rio Grande do Sul.: Relatório econômico 2012 e perspectivas para 2013, <http://www.farsul.org.br/pg_lista_arquivos.php>.

Gao, F., Morisette, J.T., Wolfe, R.E., Ederer, G., Pedelty, J., Masuoka, E., Myneni, R.B., Tan, B., Nightingale, J., 2008. An algorithm to produce temporally and spatially continuous MODIS LAI time series. IEEE Geosci. Remote Sens. Lett. 5 (1), 60–64.

Gutiérrez, A.P.A., Engle, N.L., De Nys, E., Molejón, C., Martins, E., 2014. Drought preparedness in Brazil. Weather and Climate Extremes, <http://dx.doi.org/10.1016/j.wace.2013.1012.1001i>.

Hain, C.R., Crow, W.T., Mecikalski, J.R., Anderson, M.C., Holmes, T., 2011. An intercomparison of available soil moisture estimates from thermal-infrared and passive microwave remote sensing and land-surface modeling. J. Geophys. Res. 116, D15107. http://dx.doi.org/10.1029/2011JD015633.

Hain, C.R., Crow, W.T., Anderson, M.C., Mecikalski, J.R., 2012. Developing a dual assimilation approach for thermal infrared and passive microwave soil moisture retrievals. Water Resour. Res. 48, W11517. http://dx.doi.org/10.1029/2011WR011268.

Hain, C.R., Anderson, M.C., Crow, W.T., Yilmaz, M.T., 2015. Diagnosing neglected moisture source/sink processes with a thermal infrared-based Two-Source Energy Balance model. Water Resour. Res. (in press).

Hastenrath, S., Wu, M.-C., Chu, P.-S., 1984. Towards the monitoring and prediction of north-east Brazil droughts. Quart. J. Roy. Meteorol. Soc. 110, 411–425.

Holmes, T., Crow, W.T., Hain, C.R., Anderson, M.C., Kustas, W.P., 2015. Amplitutde of the diurnal temperature cycle as observed by thermal infrared and microwave radiometers. Int. J. Remote Sens. (in press).

Huffman, G.J., Adler, R.F., Bolving, D.T., Gu, G., Nelkin, E.J., Hong, Y., Wolff, D.B., Bowman, K.P., Stocker, E.F., 2007. The TRMM Multisatellite Precipitation Analysis (TMPA): quasi-global, multiyear, combined-sensor precipitation estimates at fine scales. J. Hydrometeorol. 8, 38–55.

Jonsson, P., Eklundh, L., 2004. TIMESAT – a program for analyzing time-series of satellite sensor data. Comput. Geosci. 30, 833–845.

Leivas, J., Andrade, R., Victoria, D., Torresan, F., Bolfe, E., Barros, T., 2012. Monitoramento da seca ocorrida em 2012 no Nordeste brasileiro a partir dos dados do Spot vegetation e TRMM. <http://www.cnpm.embrapa.br/projetos/geonetcast/download/documentos/Geonordeste2012_seca2012.pdf> (in Portuguese).

Lewis, S.L., Brando, P.M., Phillips, O.L., van der Heijden, G.M.F., Nepstad, D., 2011. The 2010 Amazon Drought. Science 331, 554.

Liu, W.H., Massambani, O., Nobre, C.A., 1994. Satellite recorded vegetation response to drought in Brazil. Int. J. Climatol. 14, 343–354.

Marengo, J.A., Nobre, C.A., Tomasella, J., Oyama, M., Sampaio, G., Camargo, H., Alves, L.M., 2008. The drought of Amazonia in 2005. J. Climate 21, 495–516.

Marengo, J.A., Tomasella, J., Alves, L.M., Soares, W.R., Rodriquez, D.A., 2011. The drought of 2010 in the context of historical droughts in the Amazon region. Geophys. Res. Lett. 38, 1–5.

Marengo, J.A., Tomasella, J., Soares, W.R., Alves, L.M., Nobre, C.A., 2012. Extreme climatic events in the Amazon basin: climatological and hydrological context of recent floods. Theor. Appl. Climatol. 2012, 73–85.

Marengo, J.A., Alves, L.M., Soares, W.R., Rodriquez, D.A., 2013a. Two contrasting severe seasonal extremes in tropical South America in 2012: flood in Amazonia and drought in Northeast Brazil. J. Climate 26, 9137–9154.

Marengo, J.A., Borma, L.S., Rodriquez, D.A., Pinho, P., Soares, W.R., Alves, L.M., 2013b. Recent extremes of drought and flooding in Amazonia: vulnerabilities and human adaptation. Am. J. Climate Change 2, 87–96.

Mecikalski, J.M., Diak, G.R., Anderson, M.C., Norman, J.M., 1999. Estimating fluxes on continental scales using remotely-sensed data in an atmosphere-land exchange model. J. Appl. Meteorol. 38, 1352–1369.

Moura, A.D., Shukla, S., 1981. On the dynamics of drought in Northeast Brazil: observation, theory and numerical experiments with a General Circulation Model. J. Atmos. Sci. 38, 2653–2675.

Myneni, R.B., Yang, W., Nemani, R.R., Huete, A., et al., 2007. Large seasonal swings in leaf area of Amazon rainforests. P.N.A.S. 104, 4820–4823.

Nepstad, D.C., de Carvalho, C.R., Davidson, E.A., Jipp, P.H., Lefebvre, P.A., Negreiros, G.H., da Silva, E.D., Stone, T.A., Trumbore, S.E., Vieira, S., 1994. The role of deep roots in the hydrological and carbon cycles of Amazonian forests and pastures. Nature 372, 666–669.

Norman, J.M., Anderson, M.C., Kustas, W.P., French, A.N., Mecikalski, J.R., Torn, R.D., Diak, G.R., Schmugge, T.J., Tanner, B.C.W., 2003. Remote sensing of surface energy fluxes at 10^1-m pixel resolutions. Water Resour. Res. 39. http://dx.doi.org/10.1029/2002WR001775.

Otkin, J.A., Anderson, M.C., Hain, C.R., Mladenova, I.E., Basara, J.B., Svoboda, M., 2013a. Examining rapid onset drought development using the thermal infrared based Evaporative Stress Index. J. Hydrometeorol. 14, 1057–1074.

Otkin, J.A., Anderson, M.C., Hain, C.R., Svoboda, M., 2013b. Examining the relationship between drought development and rapid changes in the Evaporative Stress Index. J. Hydrometeorol. http://dx.doi.org/10.1175/JHM-D-13-0110.1.

Phillips, O.L., Aragao, L.E.O.C., Lewis, S.L., et al., 2009. Drought sensitivity of the Amazon rainforest. Science 323, 1344–1347.

Rienecker, M.M., Suarez, M.J., Gelaro, R., Todling, R., Bacmeister, J., Liu, E., Bosilovich, M.G., Schubert, S.D., Takacs, L., Kim, G.-K., Bloom, S., Chen, J., Collins, D., Conaty, A., da Silva, A., 2011. MERRA: NASA's modern-era retrospective analysis for research and applications. J. Climate 24, 3624–3648. http://dx.doi.org/10.1175/JCLI-D-11-00015.1.

Saleska, S.R., Didan, K., Huete, A.R., Rocha, H.R., 2007. Amazon Forests green-up during 2005 drought. Science 318, 612.

Samanta, A., Ganguly, S., Hashimoto, H., Devadiga, S., Vermote, E., Knyazikhin, Y., Nemani, R.R., Myneni, R.B., 2010a. Amazon forests did not green-up during the 2005 drought. Geophys. Res. Lett. 37, L05401. http://dx.doi.org/10.1029/2009GL042154.

Samanta, A., Ganguly, S., Myneni, R.B., 2010b. MODIS Enhanced Vegetation Index data do not show greening of Amazon forests during the 2005 drought. New Phytol. 189, 11–15.

Samanta, A., Ganguly, S., Vermote, E., Nemani, R.R., Myneni, R.B., 2012. Interpretation of variations in MODIS-measured greenness levels of Amazon forests during 2000 to 2009. Environ. Res. Lett. 7. http://dx.doi.org/10.1088/1748-9326/1087/1082/024018.

Sentelhas, P.C., Battisti, R., Câmara, G.M., Farias, J.R., Nendel, C., Hampf, A.C., 2015. Soybean yield gap in Brazil – Magnitude, causes and possible solutions for a sustainable production. Exp. Agric. (in press).

Sousa Junior, M.A., Lacruz, M.S.P., Sausen, T.M., Costa, L.F., Pereira, R.S., 2012. Estiagem na região Sul do Brasil-caracterização por meio de Imagens EVI/MODIS. In: Congresso Brasileiro Sobre Desastres Naturais. <http://www.inpe.br/crs/geodesastres/conteudo/publicacoes/Estiagem_na_Regiao_Sul_do_Brasil_Caracterizacao_Por_Meio_de_Imagens_EVI_MODIS.pdf>.

Toomey, M., Roberts, D.A., Still, C., Goulden, M.L., 2011. Remotely sensed heat anomalies linked with Amazonian forest biomass declines. Geophys. Res. Lett. 38, L19704. http://dx.doi.org/10.1029/2011GL049041.

Wardlow, B.D., Anderson, M.C., Verdin, J.P. (Eds.), 2012. Remote Sensing for Drought: Innovative Monitoring Approaches. CRC Press/Taylor and Francis, Boca Raton, FL.

Xu, L., Samanta, A., Costa, M.H., Ganguly, S., Nemani, R.R., Myneni, R.B., 2011. Widespread decline in greenness of Amazonian vegetation due to the 2010 drought. Geophys. Res. Lett. 38, L07402. http://dx.doi.org/10.1029/2011GL046824.

Yilmaz, M.T., Anderson, M.C., Zaitchik, B.F., Hain, C.R., Crow, W.T., Ozdogan, M., Chung, J.A., 2014. Comparison of prognostic and diagnostic surface flux modeling approaches over the Nile River Basin. Water Resour. Res. 50, 386–408.

Zaitchik, B.F., Simane, B., Habib, S., Anderson, M.C., Ozdogan, M., Foltz, J.D., 2012. Building climate resilience in the Blue Nile/Abay Highlands: a role for Earth System Sciences. Int. J. Environ. Res. Public Health 9, 435–461.

Zeri, M., Sá, L.D.A., Manzi, A.O., Araujo, A.C., Aguiar, R.G., von Randow, C., Sampaio, G., Cardoso, F.L., Nobre, C.A., 2014. Variabilityn of carbon and water fluxes following climate extremes over a tropical forest in southwestern Amazonia. PLoS ONE 9, 1–12.